Exact likelihood evaluations and foreground marginalization in low resolution WMAP data

Anže Slosar
Faculty of Mathemathics and Physics, University of Ljubljana, Slovenia

Uroš Seljak and Alexey Makarov
Department of Physics, Princeton University, Princeton, New Jersey 08544, USA

(Received 3 March 2004; published 18 June 2004)

The large scale anisotropies of Wilkinson Microwave Anisotropy Probe (WMAP) data have attracted a lot of attention and have been a source of controversy, with many favorite cosmological models being apparently disfavored by the power spectrum estimates at low ℓ. All the existing analyses of theoretical models are based on approximations for the likelihood function, which are likely to be inaccurate on large scales. Here we present exact evaluations of the likelihood of the low multipoles by direct inversion of the theoretical covariance matrix for low resolution WMAP maps. We project out the unwanted galactic contaminants using the WMAP derived maps of these foregrounds. This improves over the template based foreground subtraction used in the original analysis, which can remove some of the cosmological signal and may lead to a suppression of power. As a result we find an increase in power at low multipoles. For the quadrupole the maximum likelihood values are rather uncertain and vary between 140 and 220 $\mu\mathrm{K}^2$. On the other hand, the probability distribution away from the peak is robust and, assuming a uniform prior between 0 and 2000 $\mu\mathrm{K}^2$, the probability of having the true value above 1200 $\mu\mathrm{K}^2$ (as predicted by the simplest cold dark matter model with a cosmological constant) is 10%, a factor of 2.5 higher than predicted by the WMAP likelihood code. We do not find the correlation function to be unusual beyond the low quadrupole value. We develop a fast likelihood evaluation routine that can be used instead of WMAP routines for low ℓ values. We apply it to the Markov chain Monte Carlo analysis to compare the cosmological parameters between the two cases. The new analysis of WMAP either alone or jointly with the Sloan Digital Sky Survey (SDSS) and the Very Small Array (VSA) data reduces the evidence for running to less than 1σ, giving $\alpha_s = -0.022 \pm 0.033$ for the combined case. The new analysis prefers about a 1σ lower value of Ω_m, a consequence of an increased integrated Sachs-Wolfe (ISW) effect contribution required by the increase in the spectrum at low ℓ. These results suggest that the details of foreground removal and full likelihood analysis are important for parameter estimation from the WMAP data. They are robust in the sense that they do not change significantly with frequency, mask, or details of foreground template marginalization. The marginalization approach presented here is the most conservative method to remove the foregrounds and should be particularly useful in the analysis of polarization, where foreground contamination may be much more severe.

DOI: 10.1103/PhysRevD.69.123003 PACS number(s): 98.70.Vc

I. INTRODUCTION

Data analysis of cosmic microwave background maps is a challenging numerical problem. The question that we want to answer is the probability (or likelihood) of a theoretical model given the data. In order to evaluate the exact likelihood of a theoretical power spectrum of cosmic microwave background (CMB) fluctuations given a sky map of these fluctuations, it is necessary to invert the theoretical covariance matrix. This operation scales as $O(N^3)$, where N is the length of the data vector and is currently limited by practically available computer technology to $N \lesssim 10^4$. One is hence forced to use approximate estimators when inferring the power spectrum from data such as those of the Wilkinson Microwave Anisotropy Probe (WMAP) satellite [1], which have 1–2 orders of magnitude more independent measurements. The most popular methods are the pseudo-Cl (PCL) method (see, e.g., [2]) and the quadratic maximum likelihood (QML) estimator (see, e.g., [3]). Both of these methods produce as an intermediate step estimates of multipole moments C_ℓ, and approximate methods have been developed to describe their probability distributions as accurately as possible [4,5]. These perform satisfactorily for high ℓ values, where the central limit theorem guarantees that a Gaussian distribution (in offset lognormal transformed variables) will be a good approximation. Unfortunately, these methods are much less reliable at low multipoles, where the distributions are not Gaussian. The situation is complicated further by the masks applied to the data to remove the galactic foreground contamination and by the marginalization of unwanted components, all of which makes analytic approach unreliable. In [6] it was suggested to use a hybrid approach using QML on degraded maps at low ℓ and PCL at higher multipoles.

The issue of the exact values of multipole moments in WMAP data has attracted much attention since the original analysis by the WMAP team [7]. Several unusual features have already been pointed out in the original analysis. One of these was the correlation function, which appears to almost vanish above 60°. Another was the low value of the quadrupole. With the PCL analysis the value of the quadrupole was found to be $\sim 123\ \mu\mathrm{K}^2$, compared to the expected value of $\sim 1200\ \mu\mathrm{K}^2$ for the simplest cold dark matter model with a cosmological constant (ΛCDM model). The probability for this low value was estimated to be below 1%, depending on the parameter space of the models. The discussion of the statistical significance of the low values of the quadrupole

and octopole in the WMAP data [8–11] has sparked a renewed interest in the so called estimator induced variance [12]—the error in the likelihood evaluation arising due to the use of an estimator rather than the exact expression. In [12] it was argued that the QML estimator performs significantly better than the PCL estimator and that the true value of the quadrupole probably lies in the range around 170–250 μK^2. However, only the maximum likelihood value was computed and not the full likelihood distributions, so the statistical significance of this result and its effect on the parameter estimation remained unclear. In addition, the role of foregrounds and monopole/dipole removal has not been explored in detail.

In this paper we take a different approach. We argue that the actual value of the best fitted quadrupole (and other multipoles) is not of major interest, since it can be quite sensitive to the details of the foreground subtraction procedure, type of mask used, and numerical details of the analysis (in fact, the various values proposed so far may even be statistically indistinguishable if the likelihood function at the peak is very broad). What is more important is the probability or likelihood of a model given the data, compared to another model that may, for example, fit the data better. This is encapsulated in the likelihood ratio between models, and within the Bayesian context is the only information we really need to assess the viability of cosmological models that belong to a certain class. In this paper we perform the exact likelihood calculation by a direct inversion of the covariance matrix for the low resolution maps, thus eliminating all the uncertainties related to estimator variance approximations. Since we use low resolution maps with less than 3000 pixels we can do the inversions with brute force linear algebra routines. This means we cannot do the analysis on all of the multipole moments, so we analyze low multipoles with the exact method and use PCL analysis for the higher multipoles, where the two methods agree with each other and where the approximate variance estimates developed for PCL analysis are likely to be valid.

The second issue we wish to address in this paper is the question of foreground subtraction. This is done in two steps. First, pixels with a high degree of contamination are completely removed from the data. This results in the so called KP2 (less aggressive, 85% of the sky) and KP0 (more aggressive, 75% of the sky) masks [13]. There remains contamination even outside these masks in individual frequency channels. This contamination can be further reduced using templates and/or frequency information [13]. In the WMAP analysis the templates were fitted for and subtracted out of the WMAP data. Even with a perfect template there is a danger that this procedure can oversubtract the foregrounds, since one is essentially subtracting out the maximum amplitude consistent with the template, which could include some of the signal. Instead, here we do not subtract out the templates, but marginalize over them by not using any information in the data that correlates with a given template. This procedure has not been applied to the WMAP data in previous analyses. It guarantees that there is no statistical bias caused by the foreground removal.

Some of the templates that were subtracted in the WMAP analysis, particularly the 408 MHz Haslam synchrotron radiation map [14], are of poor quality. WMAP produced a better set of templates by applying the maximum entropy method (MEM) to WMAP maps in several frequency channels using templates as priors only [13]. In addition to the Haslam synchrotron map, they used [15] the H-α map as a tracer of free-free emission and the Schlegel-Finkbeiner-Davis (SFD) dust template based on [16]. This process resulted in three MEM derived foreground maps. These, however, were not used to infer the power spectrum. Instead, the official power spectrum was determined from the integrated single frequency maps and the same templates that were used as priors for the MEM map making procedure, ignoring the MEM derived maps.

The MEM derived maps are likely to be the most faithful representation of the foregrounds. When used in power spectrum inference, however, they must be used with care due to the complicated nature of their signal and noise correlations [13]. Nevertheless, on the largest scales, where receiver noise is negligible, they are probably the best available option. We therefore use the integrated single channel maps and the MEM derived foreground templates as a basis for our work. Note that in the foreground marginalization procedure no template is actually removed from the data and there is no danger of introducing noise correlations that could significantly affect the power spectrum estimates. We perform this process on foreground unsubtracted maps of the V and W channels of the WMAP satellite. We use both KP2 and KP0 masks and project out the remaining galactic contamination using MEM inferred maps of dust, synchrotron, and free-free foregrounds. We use the likelihood evaluated in this way to asses the statistical significance of departure from the concordant model at low multipoles and to perform a statistical analysis of cosmological models given the data.

The WMAP team also produced the so called internal linear combination (ILC) map of the CMB emission, by using internal maps at various frequencies to decompose them into CMB and foreground components. This approach is not based on any templates and so uses less information than is available in principle. While visually these maps appear to be relatively free of contamination outside the galactic plane, there are still artifacts within the plane. This means that one must be careful when projecting out monopoles and dipoles: one should not simply remove them from the all-sky map, since they could be contaminated by galactic emission at the center and this would leave a residual offset outside the galactic plane, which could contaminate all the low multipoles. One must again apply marginalization over monopoles and quadrupoles on the masked map to eliminate any contamination in the final result. A similar approach has been taken by [17] and [18], who produced their own versions of ILC maps. Since we argue that the best method is to use single frequency maps together with correct templates and we use the ILC map for illustration and cross-check purposes only, we do not consider these alternative ILC solutions further.

II. METHOD

A. Likelihood evaluation

Given noiseless and independent measurements of the CMB sky **d**, the theoretical covariance matrix for these measurements is given by [19]

$$C_{i,j}=\sum_{\ell=2}^{\infty}\frac{2\ell+1}{4\pi}C_\ell P_\ell(\cos\theta_{i,j}), \quad (1)$$

where C_ℓ is the power spectrum, P_ℓ is the Legendre polynomial of order ℓ, and $\theta_{i,j}$ is the angle between the ith and jth points on the sky. We also define

$$\mathsf{C}_\ell=\frac{C_\ell\ell(\ell+1)}{2\pi}, \quad (2)$$

which is the quantity that is conventionally plotted (and often referred to) as the power spectrum.

In addition to the covariance matrix in Eq. (1) we want to project out linear components of the data vector that correspond to known contaminants in our data. Fortunately, there exists a standard procedure for this [20]: the covariance matrix of the contaminant is calculated and added to the theoretical covariance matrix with a very large variance. Here the covariance matrix of the template is given by $\mathrm{C}=\langle\mathbf{L}\mathbf{L}^\dagger\rangle$, where $\mathbf{L}$ is the template vector. Using this method, we project out the map's monopole and dipole and the known galactic contaminants, namely, dust, synchrotron, and free-free emission. For completeness we add the diagonal noise component $N_{ii}=\sigma_i^2$, although this is not strictly required for this analysis, because the noise power spectrum is below 10 $\mu\mathrm{K}^2$ on the scales of our interest.

Hence, the total covariance matrix can be written as

$$\mathbf{C}^{\mathrm{total}}=\mathbf{C}+\mathbf{N}+\lambda(\mathbf{C}^{\mathrm{dust}}+\mathbf{C}^{\mathrm{synch}}+\mathbf{C}^{\mathrm{free\text{-}free}}\mathbf{C}^{\ell=0}+\mathbf{C}^{\ell=1}). \quad (3)$$

The value of λ in the above equation must be large enough so that unwanted components are projected out. If it is too large, however, the numerical errors start to affect the results.

The logarithm of the likelihood of given C_ℓ's can then be written as

$$\log L=-\frac{1}{2}\mathbf{d}^{\mathbf{T}}(\mathbf{C}^{\mathrm{total}})^{-1}\mathbf{d}-\frac{1}{2}(\log|\mathbf{C}|+N\log 2\pi), \quad (4)$$

where $\mathbf{d}$ is the data vector. To evaluate the likelihood of a given theoretical model we simply evaluate this expression, computing the covariance matrix using the theoretical model spectrum C_ℓ in Eq. (1).

B. Choice and preparation of maps

As mentioned in the Introduction, the procedure described above can realistically be performed only on modestly sized maps. We decrease the resolution of a given map using the following procedure. First, the full resolution source map is multiplied by the mask, whereby every masked pixel is zeroed, while unmasked pixels remain the same. The map is then smoothed by the 5° full width at half maximum Gaussian beam and resampled at a lower HEALPIX [21] resolution (NSIDE=16), giving 3072 roughly independent pixels on a full-sky map. The mask itself is smoothed in the same manner, and this tells us by how much the smoothed pixels that were affected by the mask need to be upscaled. We do not use pixels whose smoothed mask value drops below 0.7. We use this information to reduce the effective scale of the smoothing beam (by the square root of this correction) in the calculation of the covariance matrix, although we verified that this does not affect any of the final results.

We have also attempted an exact calculation of the window function by treating each subpixel of a low resolution HEALPIX map separately. Unfortunately, this is computationally prohibitively expensive. Instead, we performed weighted averaging within each low resolution HEALPIX pixel using the effective HEALPIX window function provided with the package and get compatible results. We chose not to adopt this approach for the main analysis since the individual HEALPIX pixel windows are anisotropic, depend on the mask, and are very slowly decreasing with increasing ℓ. For our resolution level the effective windows (which are valid only for full sky coverage) are given only up to $\ell=64$, and there is still a lot of power beyond that.

The Gaussian smoothing procedure was used on WMAP integrated maps for the V and W channels and for the MEM maps for the three major foregrounds: dust, synchrotron, and free-free emission. In all cases, the low resolution maps were produced for the KP2 mask and for the more conservative KP0 mask. We also applied the same procedure to the ILC map, except that in this case we smoothed over the whole map and so did not need to upscale the pixel values by the effect of the mask. By changing various parameters of the inversion process we got consistent likelihoods, and we estimate the uncertainty in likelihood evaluation to be about 0.2 in logarithm of the likelihood.

III. MULTIPOLE MOMENTS AND THEIR STATISTICAL SIGNIFICANCE

In Fig. 1 we show the maximum likelihood (ML) values of the multipoles up to $\ell=18$ for several of our basic cases. One can see from this figure that most of the estimates up to $\ell\sim10$ are above the PCL values given by the WMAP team, while at higher multipoles the two agree well ($\ell=11$ appears anomalous and PCL gives a much higher value than the exact likelihood analysis). Some of the differences are due to random fluctuations: KP2 mask contains 85% of the sky compared to 75% for KP0 and this can lead to differences in the two estimates. Similarly, projecting out the foreground templates reduces the amount of information, so there can be statistical differences between our analysis and one without marginalization. While the differences between KP0 and KP2 masks are likely to be within the allowed range of statistical fluctuations, this is less likely for the differences between WMAP PCL and our analysis of V with the KP2 mask, since the same mask and channel were used by WMAP. The difference is partly due to the use of the exact likelihood analysis and partly due to the foreground marginalization. While the WMAP team marginalized over monopoles and dipoles, they subtracted out the foregrounds with the maximal amplitude, which may have removed some of the true cosmological signal and pushed the values lower. To eliminate the bias that can arise from this procedure, it is best

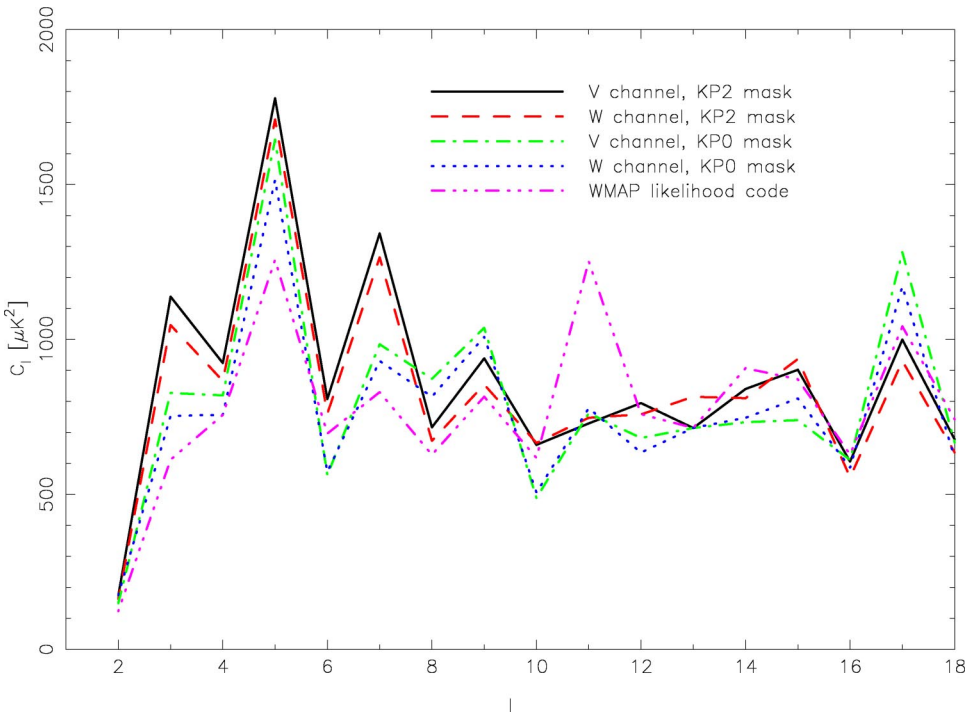

FIG. 1. This figure shows the maximum likelihood power spectrum for several combinations of frequencies and masks. Note that all spectra agree reasonably well beyond $\ell = 11$.

to exclude the information in the signal that correlates with templates and with monopoles or dipoles. This reduces the statistical power but is guaranteed to be unbiased.

To investigate further the robustness of our results, Fig. 2 shows the most likely values of power spectra (up to multipole $\ell = 10$) for various combinations of template choice for the W channel data and for the ILC map. This realistically indicates potential systematic differences arising due to the choice of templates. On the same graphs we also show the reduction performed with HEALPIX window functions (where pixels of the low resolution map were only weighted averages of all corresponding pixels in the high resolution map), indicating that our results are robust with respect to the choice of window function and smoothing procedure. The differences between the various cases are small compared to the difference between exact evaluations and WMAP values. We emphasize that the ML values are the least robust part of the analysis, and it is much more important that the probability distributions away from the peak are consistent. For the quadrupole we discuss this below, while the overall impact

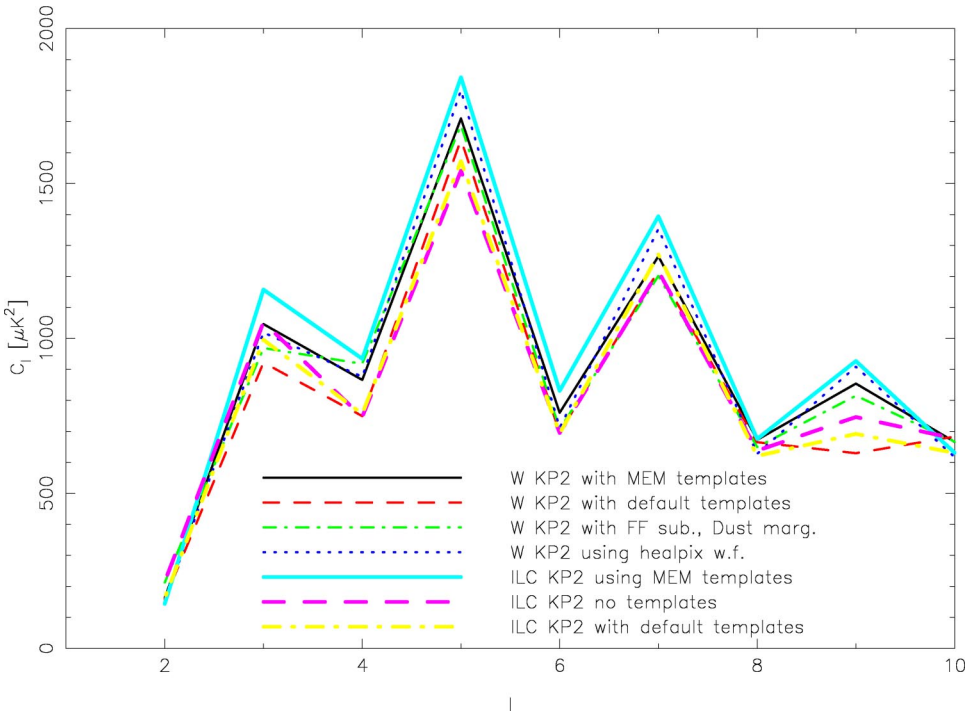

FIG. 2. This figure shows the maximum likelihood power spectrum up to $\ell = 10$ for several test cases. The derived features in the most likely values of power spectrum are robust with respect to choice of window function (Gaussian versus HEALPIX), templates (MEM versus external, dust only versus standard three templates in W), and maps (W versus ILC).

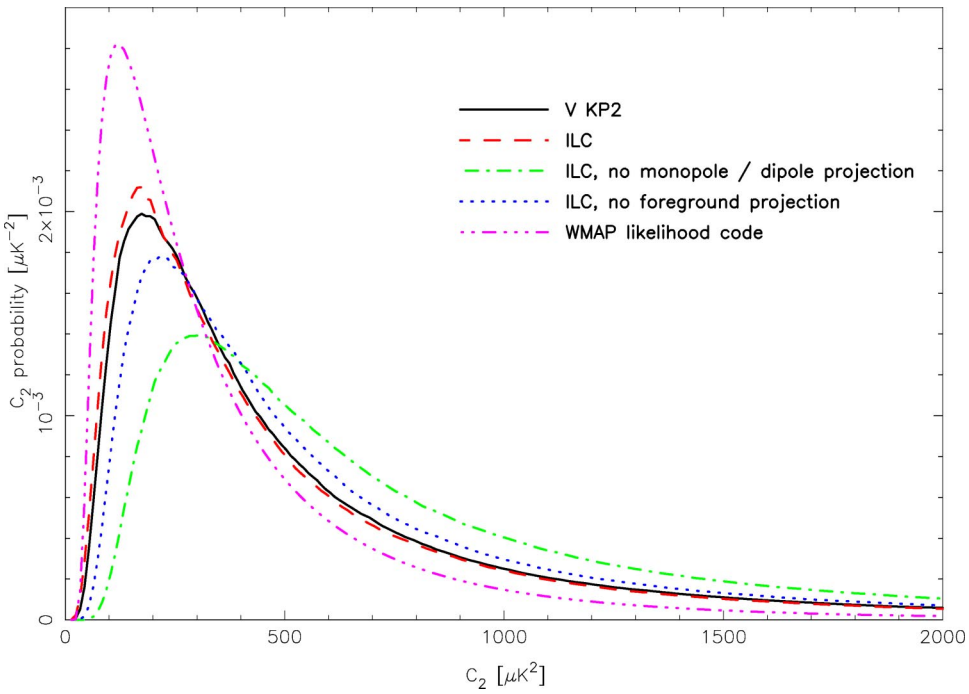

FIG. 3. This figure shows the probability distributions for the value of C_2 as inferred for the various combinations of the monopole and dipole and the foreground marginalization. Also shown is the official WMAP likelihood code output. Note that C_2 in V without the monopole and dipole or the foreground marginalization is heavily contaminated and gives very high ML values, while all the other cases have very similar probability distributions (except the WMAP code).

on the cosmological parameter estimation is discussed in the next section.

The marginalization procedure is guaranteed to give unbiased results independent of the form of the template or its non-Gaussian properties. The only assumption is that the template is not correlated with the true CMB, which could happen if the templates were produced from the CMB data themselves and were affected by noise, calibration, or beam uncertainties. It is unlikely that this would happen on large scales. We have tested this hypothesis by using the external templates instead of the MEM templates, without finding much difference in the result (Fig. 2).

Figure 3 shows the probability distribution for the value of C_2 for several cases, assuming the best fit ΛCDM model for other C_ℓ's. The particular choice of other C_ℓ's affects the inferred curves, although at a level below the variance between various curves. It has several interesting features. First, when all marginalizations are used, the V channel, W (not shown), and ILC give very consistent results. In the absence of marginalization and foreground subtraction the V and W channel maps are very affected by the foregrounds and the ML values reach up to 500 μK^2. The ILC map could be affected by the foreground marginalization; its value drops from $\sim$220 μK^2 (consistent with [12]) to $\sim$170 μK^2 when projection is included in the analysis. The ILC map may suffer even more from the residual monopole/dipole contamination, which pushes the quadrupole value up.

While our procedure of marginalizing over three templates is the most conservative, one may worry that it is unnecessary. Some of the channels are not really strongly contaminated by all three components and if frequency scaling is known then multifrequency information can be used to constrain a given component in a given channel. While there is nothing wrong with our procedure one could argue that it reduces the amount of information. The number of eliminated modes is roughly given by the number of templates used, but since the templates are correlated (being all dominated by our galaxy) the information loss from large scale modes is likely to be less than three. It is also not clear how the templates couple to different multipoles. To test these effects we perform the analysis in the W channel, where foreground contamination is dominated by dust. We use marginalization only over the SFD dust template (subtracting out the free-free component and doing nothing for the synchrotron). We find that this has very little effect on the maximum likelihood values of multipoles, as shown in Fig. 2. For $\ell=2$ we find the ML value at 220 μK^2, slightly higher than in other cases (Fig. 4), but the overall probability distribution is very similar to other cases. The effect of this procedure on the parameter estimation is explored in the next section.

It is interesting to assess the statistical significance of the departure of the lowest multipoles from the concordant model. Our focus is not on the actual statistical procedure of assessing this departure (see, e.g., [8]), but on the effect of estimator induced variance. We consider five cases: all possible combinations of the choice of mask (KP2 or KP0) and frequency (V channel or W channel) and the official WMAP likelihood code [5,22]. The inferred maximum likelihood values (Fig. 4) lie in the range 140 μK^2–220 μK^2, but the likelihood function is broad at the peak and the exact value of the maximum likelihood estimate is driven by small details in the analysis: in all of our basic cases the likelihood is within 10–20 % of the peak value over the range 120–250 μK^2. Thus our results are consistent with both the original WMAP value (123 μK^2) and the values in [12] and there is no ''correct'' value given the level of foreground contamination.

As we argued in the Introduction, the precise value of the maximum likelihood estimator is not of primary interest, given that it can be strongly affected by the details of the analysis. Much more important for the question of parameter estimation is the shape of the likelihood function. Figures 3

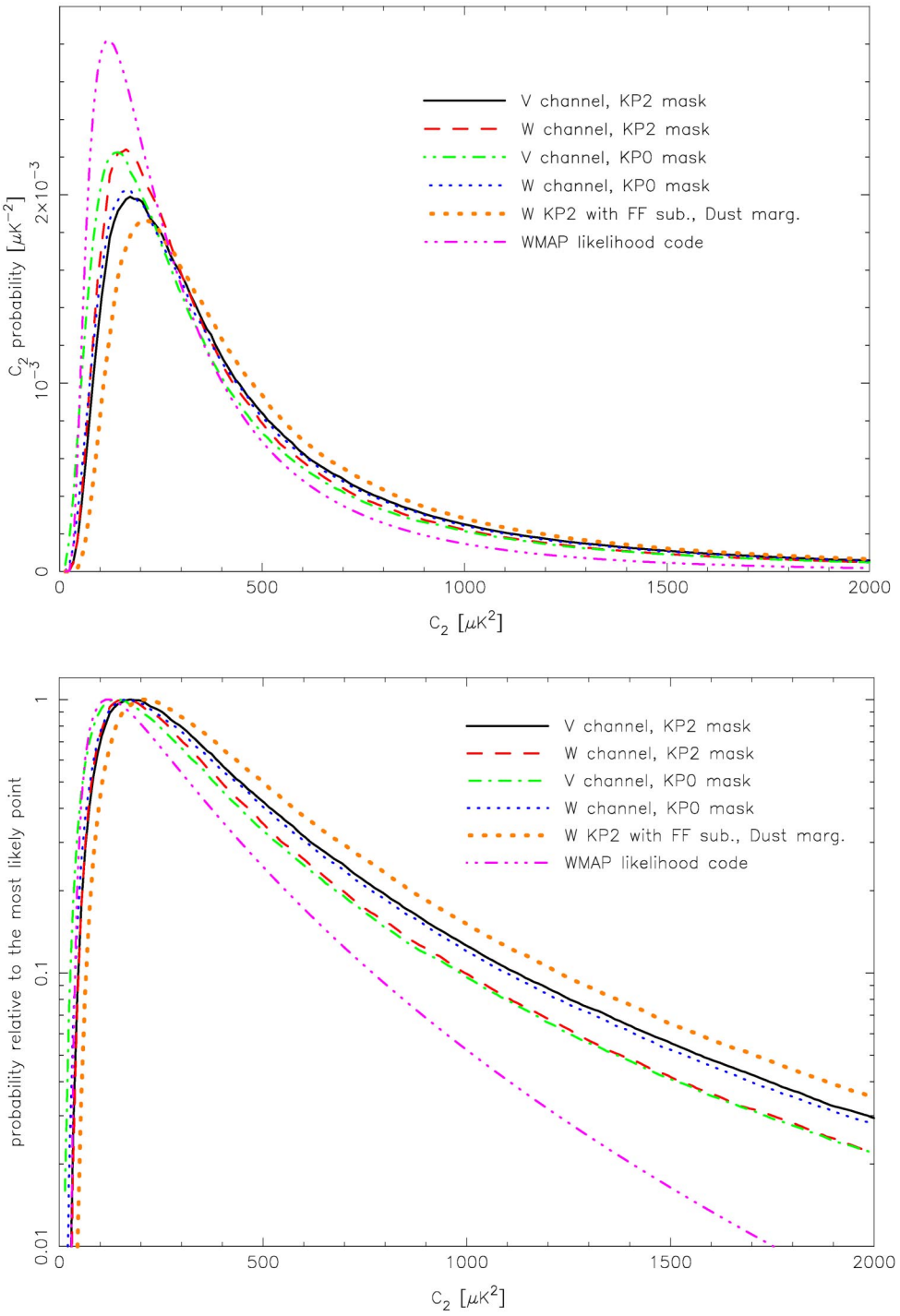

FIG. 4. This figure shows the probability distributions for the value of C_2 as inferred for the various combinations of the selected channel and mask and the official WMAP likelihood code. The upper panel shows the normalized probability distribution, while the lower panel shows the probability relative to the most likely point. Note that the lower panel's vertical axis is logarithmic. Values of other C_ℓ's were set to those of the best fit ΛCDM model.

and 4 show that, while the maximum likelihood value of the quadrupole is quite uncertain, all our cases give very similar shapes of the likelihood function. This likelihood distribution is not consistent with the likelihood provided by the WMAP team, which appears to underestimate the errors associated with the galactic cut and marginalizations. The WMAP likelihood of the concordant model C_2 ($\sim 1200\ \mu K^2$) is roughly 2.5 times too low with respect to the most likely point when compared to our likelihood values. This change in the shape of the likelihood function affects the parameter estimation, particularly the running of the spectral index, as shown in Sec. IV. We note here that not performing the marginaliza-

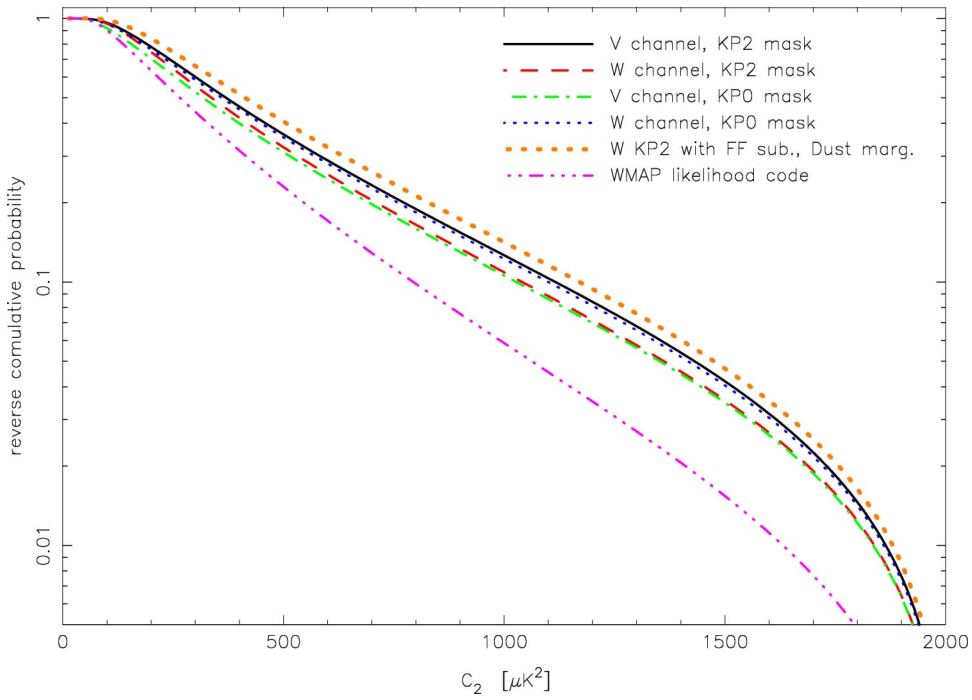

FIG. 5. Cumulative probability as a function of the true value of the quadrupole (integrated from large values downward assuming $0<C_2<2000\ \mu K^2$).

tion over foregrounds and/or the monopole and dipole would lead to an even higher probability of the concordance model compared to low C_2 models (see the corresponding probability distributions in Fig. 3), but these are more likely to be contaminated and should not be used in the likelihood analysis.

Figure 5 shows the integrated probability as a function of the true value of the quadrupole (integrated from large values downward), under the assumption that the prior distribution of quadrupole values is uniform between 0 and 2000 μK^2. This prior is adopted due to the fact that the concordance value of the quadrupole is $\sim 1000\ \mu K^2$ (see, e.g., [8]). This gives the probability of the true value exceeding C_2 assuming this prior. We find that this probability is around 10%, as opposed to 4% by the WMAP likelihood analysis. Thus with a uniform prior on values of C_2 the probability of the true quadrupole to be above that predicted by the concordance model is not particularly small. It becomes even larger if the upper limit at 2000 μK^2 is removed, in which case we find 18% probability of the true value exceeding the concordance value.

Note that the WMAP team chose to give the statistical significance of the low quadrupole in terms of the number of random realizations of theoretical models in Monte Carlo Markov chains (MCMCs) for which the extracted quadrupole is lower than the observed value of 123 μK^2. This is a frequentist statistic which cannot be directly compared to the one we defined here in the context of Bayesian statistics. The frequentist approach leads to lower numbers (less than 1%, compared to 4% above) for the specific value of the quadrupole obtained by WMAP, but the probability is likely to be higher if our analysis procedure is applied to the data, given our broader likelihoods and higher values of the best fitted quadrupole. The WMAP analysis does not include the uncertainties in the foreground subtractions, which should have an important effect given the skewed nature of the probability distributions: if an error estimate of 50 μK^2 on C_2 were added to the measured value, it would lead to an increased probability of the concordance model. In order to truly decouple the cosmic variance uncertainty for the errors arising from the galactic cut and foregrounds one would need to infer the probability distribution for a particular realization of $a'_{\ell m}$'s. For a full-sky CMB observation with no galactic contamination, this would be a delta function; the galactic cut and large scale contamination would spread the probability over a finite region. This distribution, marginalized to produce $p(\langle a^2_{2m}\rangle_m)$, would be the correct quantity that must be compared to the concordant value and the corresponding cosmic variance. Work on this front is currently in progress.

While the frequentist approach does allow one to test a model (or a class of models) independent of other models, it is still not free of assumptions. Testing the quadrupole on its own makes sense only if we believe that there is something special about it, for example, because it is sensitive to the physics on the largest scales, which may not be probed by lower multipoles. If it is not viewed as special, but only one of the many estimated multipoles, then the probability of one of them being this low is significantly higher. This is tested in the frequentist approach with the goodness of fit (χ^2), which for the WMAP data does not reveal any particular anomalies. Unfortunately, there is no hope of resolving these statistical questions completely with only one observed sky.

In Fig. 6 we plot the contour plots of parameters on the C_2-C_3 plane for the considered models. This shows that the likelihoods between C_2 and C_3 are only weakly correlated, both for the exact likelihood evaluation as well as for the PCL approximation. In the original analysis there was some evidence for both C_2 and C_3 being low, so that the overall significance was between 2σ and 3σ (Fig. 6). The evidence

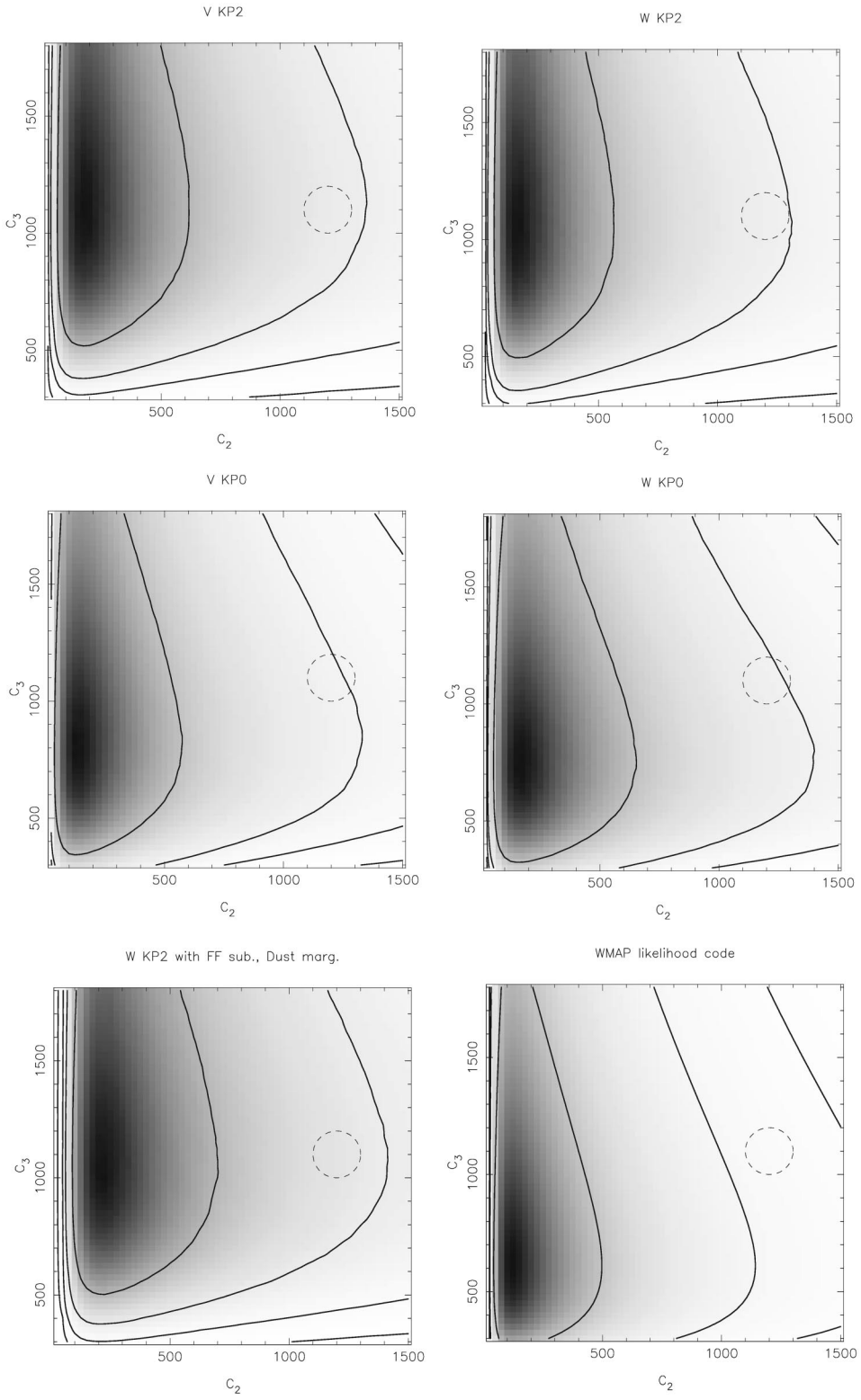

FIG. 6. In this figure we show the probability distribution function on the C_2-C_3 plane for all considered possibilities and the original WMAP likelihood code. Contours correspond to the 1σ, 2σ, 3σ, and 4σ assuming top-hat priors on the plotted limits ($0<C_2<1500\ \mu K^2$, $300<C_2<1800\ \mu K^2$). The dashed circles correspond to the approximate values of the concordant model.

for discrepancy weakens below 2σ with our analysis and is consistent among the four cases.

The WMAP team presented further evidence of the unusual nature of large scale correlations using the correlation function, which appears to vanish at angles above 60° [7]. Correlation functions are notoriously difficult to interpret due to the correlated nature of the values at different angles, so one must be careful not to overinterpret such results. In Fig. 7 we show the correlation function analysis for these cases, compared to the original WMAP analysis and to theoretical predictions of the ΛCDM model. We also show the result for the ΛCDM model where C_2 has been lowered to 150 μK^2,

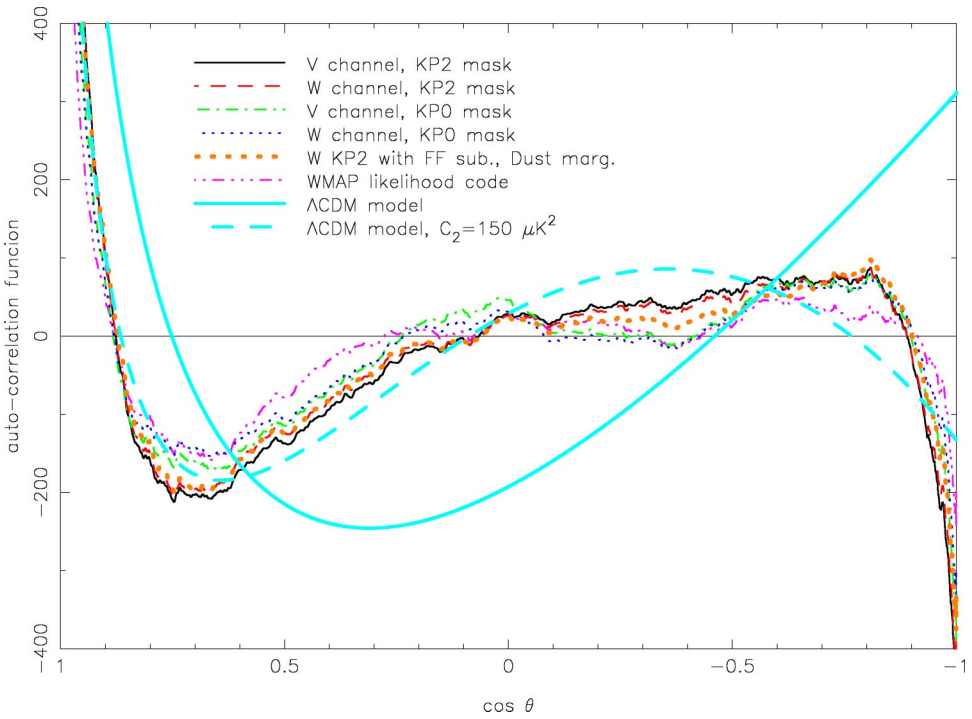

FIG. 7. This figure shows the autocorrelation function for all considered cases, the ΛCDM model favored by the WMAP data, and the same model with C_2 set to 150 μK^2.

keeping the other multipoles unchanged. Several features are apparent from this figure. First, theoretical predictions for the large scale correlation function are largely driven by the quadrupole, and lowering its value to 150 μK^2 brings the correlation function into a significantly better agreement with the observations than the unmodified ΛCDM model. Second, our results significantly modify the predicted correlation function and the deviations from zero at large angles are now much more evident, both in the positive direction and in the negative direction at very large angles. To investigate it further the WMAP team introduced a statistic $S=\int_{-1}^{0.5}[C(\theta)]^2 d\cos\theta$. This is a posterior statistic that was designed to maximize the effect, so its statistical significance is difficult to evaluate. We find that its value increases from 1691 for WMAP analysis to 4197 (W KP0), 5423 (V KP0), 9086 (V KP2), 7698 (W KP2), and 5832 (W KP2, dust marginalization only). While its value for the standard ΛCDM model is 49625, reducing the quadrupole to 150 μK^2 changes this to 8178, below the value we find in the case of V KP2. We conclude that there is no obvious anomaly in the correlation function beyond the fact that the quadrupole is low, and there is no evidence of the correlation function vanishing at large angles.

IV. PARAMETER ESTIMATION

In order to assess the effect of the exact likelihood evaluations on the inferred cosmological parameters we have run the Markov chain Monte Carlo parameter estimations using the original WMAP likelihood code and the code modified to use the exact calculations at lowest multipoles. The total likelihood was calculated by evaluating the likelihood for the $\ell \leqslant 12$ multipoles using the exact matrix inversion and adding the likelihood evaluated from the remaining multipoles using the WMAP likelihood code. The power spectrum values for the multipoles $\ell > 12$ in the exact likelihood code were kept at the WMAP PCL most likely model when calculating the covariance matrix: this ensures that the likelihood is not "accounted for" twice. We also neglect the anticorrelation between the $\ell = 12$ and $\ell = 13$ modes at the boundary. The evaluation of the exact likelihood typically takes around a few seconds on a modern workstation, and this is less than the time it takes to evaluate a theoretical CMB power spectrum with CMBFAST [23]. Therefore, using the exact likelihood code does not slow down the MCMC parameter estimation significantly. Each of the chains described below contains 100000–200000 chain elements, the success rate was of order 30–60 %, correlation length 10–30, and effective chain length of order 5000–15000. We use 8–24 chains and in terms of Gelman and Rubin $\hat{R}$ statistics [24] we find the chains are sufficiently converged and mixed with $\hat{R} < 1.01$, compared to the recommended value $\hat{R} < 1.2$ or the more conservative value $\hat{R} < 1.1$ adopted by the WMAP team [5].

The likelihood also uses the information contained in the temperature-polarization (TE) cross-correlation power spectrum using the official WMAP likelihood code, which uses similar approximations as the temperature power spectrum and completely ignores correlations between the TT and TE power spectra. We cannot yet use the exact evaluations since the polarization maps are not publicly available at this time.

We ran several MCMCs using a custom developed software described in [25]. We consider only flat models. We begin with the simplest five-parameter models

$$\mathbf{p} = (\tau, \omega_b, \omega_{\rm CDM}, \mathcal{R}, \Omega_m), \tag{5}$$

where τ is the optical depth, $\omega_b = \Omega_b h^2$ is proportional to the baryon to photon density ratio, $\omega_{\rm CDM} = \Omega_{\rm CDM} h^2$ is propor-

TABLE I. Median value and 1σ and 2σ constraints on cosmological parameters for various MCMCs based on WMAP data alone. ''5p'' denotes varying five basic cosmological parameters in MCMCs, while ''8p'' stands for eight-parameter chains. ''Old'' stands for the evaluation of the WMAP likelihood using the current WMAP provided software, VKP2 is our new exact likelihood evaluation analysis of V maps using KP2 mask, and VKP0 is the same for KP0 mask.

	5p old	5p VKP2	5p VKP0	8p old	8p VKP2
$10^2\omega_b$	$2.40^{+0.06\ +0.12}_{-0.06\ -0.13}$	$2.38^{+0.06\ +0.13}_{-0.07\ -0.13}$	$2.39^{+0.06\ +0.13}_{-0.06\ -0.13}$	$2.37^{+0.17\ +0.35}_{-0.16\ -0.32}$	$2.49^{+0.19\ +0.39}_{-0.17\ -0.34}$
Ω_m	$0.29^{+0.08\ +0.16}_{-0.06\ -0.11}$	$0.24^{+0.07\ +0.15}_{-0.05\ -0.10}$	$0.26^{+0.07\ +0.16}_{-0.06\ -0.11}$	$0.20^{+0.07\ +0.16}_{-0.06\ -0.10}$	$0.15^{+0.06\ +0.13}_{-0.04\ -0.07}$
$\omega_{\rm CDM}$	$0.12^{+0.017\ +0.03}_{-0.017\ -0.03}$	$0.11^{+0.016\ +0.03}_{-0.016\ -0.03}$	$0.11^{+0.017\ +0.03}_{-0.016\ -0.03}$	$0.10^{+0.017\ +0.03}_{-0.017\ -0.03}$	$0.09^{+0.016\ +0.03}_{-0.015\ -0.03}$
τ	$0.17^{+0.04\ +0.08}_{-0.04\ -0.09}$	$0.21^{+0.04\ +0.07}_{-0.04\ -0.08}$	$0.19^{+0.04\ +0.08}_{-0.04\ -0.08}$	$0.23^{+0.05\ +0.07}_{-0.08\ -0.16}$	$0.24^{+0.05\ +0.06}_{-0.08\ -0.17}$
σ_8	$0.94^{+0.07\ +0.13}_{-0.08\ -0.17}$	$0.90^{+0.08\ +0.15}_{-0.09\ -0.19}$	$0.92^{+0.08\ +0.15}_{-0.09\ -0.19}$	$0.81^{+0.12\ +0.25}_{-0.13\ -0.26}$	$0.75^{+0.13\ +0.24}_{-0.13\ -0.25}$
h	$0.72^{+0.05\ +0.10}_{-0.05\ -0.08}$	$0.75^{+0.05\ +0.11}_{-0.05\ -0.09}$	$0.73^{+0.05\ +0.11}_{-0.05\ -0.09}$	$0.78^{+0.08\ +0.19}_{-0.07\ -0.13}$	$0.87^{+0.09\ +0.19}_{-0.08\ -0.15}$
T/S	0	0	0	<0.76 (95%)	<0.81 (95%)
n_s	1	1	1	$0.95^{+0.07\ +0.14}_{-0.07\ -0.15}$	$1.02^{+0.07\ +0.15}_{-0.07\ -0.15}$
α_s	0	0	0	$-0.08^{+0.05\ +0.10}_{-0.06\ -0.13}$	$-0.04^{+0.05\ +0.10}_{-0.06\ -0.13}$

tional to the cold dark matter to photon density ratio, $\Omega_m = \Omega_{\rm CDM} + \Omega_b = 1 - \Omega_\lambda$ is the matter density today, and $\mathcal{R}$ is the amplitude of curvature perturbations at $k = 0.05$/Mpc (we replace this parameter with σ_8 in Table I). To reduce the degeneracies we use ω_b, $\omega_{\rm CDM}$, the angular diameter distance Θ_s, $\ln\mathcal{R}$ and $\ln\mathcal{R} - \tau - 0.5\log(\omega_b + \omega_{\rm CDM})$ instead of the parameters in Eq. (5), adopting broad flat priors on them. Most of these priors are not important because the parameters are well determined. The exception is optical depth, for which we additionally apply $\tau < 0.3$ on some of the MCMCs following the WMAP team.

The simple five-parameter model is sufficient to obtain a good fit to the WMAP data. We add CBI + ACBAR to the WMAP data [26,27] and follow the WMAP team in denoting this data set as WMAPext. The second set of MCMCs we ran was also based on the WMAPext data, but with an expanded set of parameters which include the primordial slope n_s, its running $\alpha_s = dn_s/d\ln k$, and tensors (parametrized with $r = T/S$), adopting flat priors on these parameters. Adding these three parameters improves χ^2 only by 5, so they are not really needed to improve the fit to the data. Because of this we find significant degeneracies among many of the parameters. The best fitted values are not necessarily very meaningful and they could be significantly influenced by the assumed priors, but we can still compare the changes between the new and original analysis. A third set of MCMCs was based on the combined WMAPext + SDSS analysis [28], which breaks some of these degeneracies. The last set of MCMCs was based on WMAP + VSA [29], both with and without SDSS. We remove the $\tau < 0.3$ constraint for this case. The results are shown in Tables I and II.

A. Matter density

In five-parameter chains Ω_m is the parameter that changes most by the new analysis. Its probability distribution from various MCMCs is shown in Fig. 8. This parameter is not well determined from the CMB data, since it only weakly affects the positions of acoustic peaks in a flat universe. This leaves the integrated Sachs-Wolfe effect on large scales as an important way to constrain Ω_m: reducing Ω_m leads to a decay in the gravitational potential, which increases the contribution to the large scale anisotropies from the line of sight integration of the time derivative of gravitational potential. The increase of the low multipoles by our analysis (Fig. 8) thus requires a lower value of Ω_m to fit the data. This is more prominent for KP2, where the best fit value is $\Omega_m = 0.24^{+0.07}_{-0.05}$, than for KP0 which gives $\Omega_m = 0.26^{+0.07}_{-0.06}$, but the latter contains less area and its error distribution is slightly broader. Lower Ω_m values are also preferred in the joint WMAPext + SDSS analysis, but here the SDSS data tend to push the overall value up to $\Omega_m = 0.27^{+0.05}_{-0.03}$. In these eight-parameter chains the WMAP χ^2 is higher by about 5 compared to the WMAP without SDSS. Thus there is a bit of a tension between the SDSS data, favoring high Ω_m and the WMAP data favoring low values of this parameter, although the statistical significance of this tension is low. For low $\Omega_m = 0.24$ the Hubble parameter is $h = 0.75$, still in agreement with the Hubble Space Telescope (HST) key project value of $h = 0.72 \pm 0.08$ [30]. If we eliminate tensors from the analysis then we find $\Omega_m = 0.30^{+0.06}_{-0.05}$ for a WMAP + SDSS + VSA combination of the data. The overall conclusion is that values of Ω_m between 0.2 and 0.4 remain acceptable by the data and that the actual value depends strongly on the choice of parameter space.

TABLE II. Same as Table I for WMAP+SDSS [eight-parameter MCMCs with regular (old) or corrected (exact likelihood) analysis]. The new analysis uses V KP2 with full marginalization and W KP2 with dust marginalization only. We also give WMAP+SDSS+VSA (seven-parameters). For the latter case we do not impose $\tau<0.3$.

	8p SDSS+old	8p SDSS+VKP2	8p SDSS+WKP2	7p SDSS+VSA+VKP2
$10^2\omega_b$	$2.40^{+0.16\ +0.32}_{-0.16\ -0.30}$	$2.48^{+0.16\ +0.30}_{-0.16\ -0.31}$	$2.47^{+0.16\ +0.31}_{-0.16\ -0.30}$	$2.34^{+0.18\ +0.52}_{-0.15\ -0.28}$
Ω_m	$0.31^{+0.06\ +0.13}_{-0.05\ -0.08}$	$0.27^{+0.05\ +0.11}_{-0.03\ -0.06}$	$0.28^{+0.05\ +0.11}_{-0.04\ -0.07}$	$0.30^{+0.06\ +0.12}_{-0.05\ -0.10}$
$\omega_{\rm CDM}$	$0.128^{+0.009\ +0.019}_{-0.008\ -0.016}$	$0.121^{+0.008\ +0.017}_{-0.007\ -0.014}$	$0.123^{+0.008\ +0.017}_{-0.007\ -0.014}$	$0.123^{+0.008\ +0.017}_{-0.008\ -0.018}$
τ	$0.20^{+0.07\ +0.09}_{-0.08\ -0.14}$	$0.20^{+0.07\ +0.09}_{-0.08\ -0.14}$	$0.20^{+0.07\ +0.09}_{-0.08\ -0.14}$	$0.19^{+0.11\ +0.26}_{-0.08\ -0.13}$
σ_8	$0.98^{+0.08\ +0.16}_{-0.09\ -0.16}$	$0.97^{+0.09\ +0.16}_{-0.09\ -0.16}$	$0.97^{+0.09\ +0.16}_{-0.09\ -0.16}$	$0.93^{+0.12\ +0.29}_{-0.08\ -0.13}$
h	$0.70^{+0.05\ +0.09}_{-0.05\ -0.09}$	$0.73^{+0.04\ +0.08}_{-0.04\ -0.09}$	$0.73^{+0.04\ +0.08}_{-0.04\ -0.09}$	$0.70^{+0.05\ +0.14}_{-0.05\ -0.08}$
T/S	<0.46 (95%)	<0.46 (95%)	<0.47 (95%)	0
n_s	$0.97^{+0.06\ +0.11}_{-0.06\ -0.12}$	$1.01^{+0.05\ +0.10}_{-0.06\ -0.11}$	$1.02^{+0.05\ +0.10}_{-0.06\ -0.11}$	$0.97^{+0.06\ +0.16}_{-0.06\ -0.11}$
α_s	$-0.060^{+0.038\ +0.074}_{-0.039\ -0.083}$	$-0.015^{+0.036\ +0.072}_{-0.037\ -0.080}$	$-0.032^{+0.036\ +0.072}_{-0.038\ -0.080}$	$-0.022^{+0.034\ +0.069}_{-0.032\ -0.062}$

B. Running

Running has attracted a lot of attention ever since the WMAP team argued for a 2σ evidence of negative running. When analyzing the CMB data alone one finds that running is strongly correlated with the optical depth τ. Figure 10 shows an example of this in WMAP+VSA MCMCs. We see that this particular combination of data prefers $\tau>0.3$ and that such a high value of optical depth requires large negative running. A similar effect has been noticed in WMAP+CBI analysis [31] and WMAP+VSA analysis [32]. We find that the statistical significance of running is strongly affected by the adopted prior on τ. In fact, when the prior on τ is relaxed, the one-dimensional marginalized probability distribution seems to prefer models with high values of τ and large negative running. However, we note that this is the result of the large posterior probability volume in this region, rather than a better fit to the data. Moreover, such high values of optical depth are difficult to reconcile with the hierarchical models of structure formation and would require a lot of small scale power, contrary to the effect of a negative running. Even more importantly, a high optical depth would lead to a large signal in the WMAP *EE* polarization spectrum. To

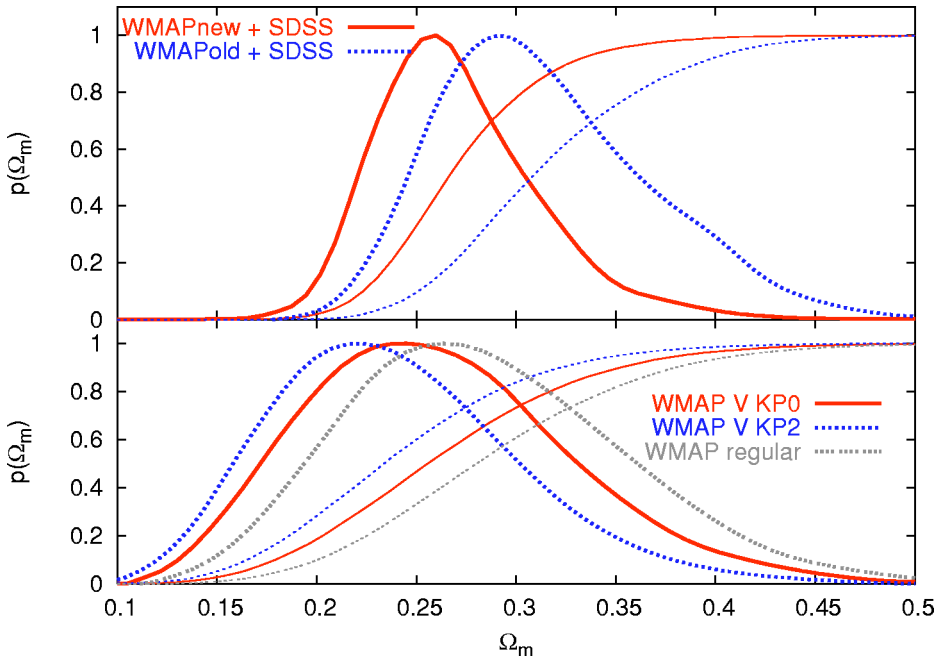

FIG. 8. Probability distribution $p(\Omega_m)$ and its cumulative value $\int_{-\infty}^{\Omega_m} p(\Omega_m')d\Omega_m'$ for five-parameter MCMCs of WMAPext data (bottom) and for eight-parameter MCMCs of WMAPext +SDSS data (top). We present V frequency map and both KP0 and KP2 mask results for the full likelihood analysis of five-parameter MCMCs of WMAPext data and V KP2 for full likelihood analysis of eight-parameter MCMCs of WMAPext+SDSS data. Also shown for comparison are the results using the regular (old) WMAP analysis routine.

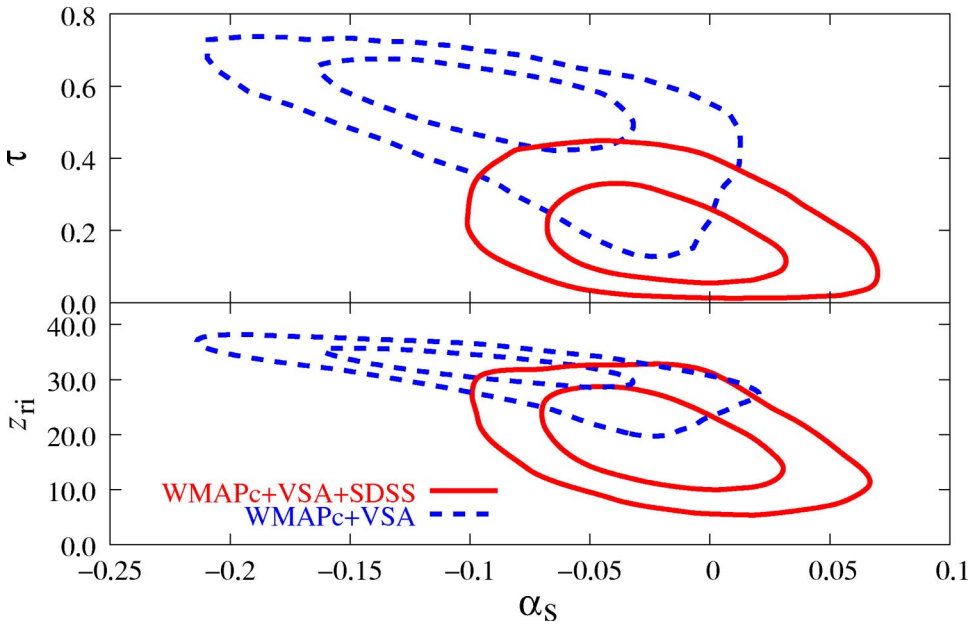

FIG. 9. Probability distribution $p(\alpha_s)$ and its cumulative value $\int_{-\infty}^{\alpha_s} p(\alpha_s')d\alpha_s'$ for old and new MCMCs using WMAPext + SDSS data. We use V frequency map and KP2 mask in the full likelihood analysis.

eliminate this region of parameter space the WMAP team adopted a prior $\tau<0.3$ and we follow that for most of our MCMCs. However, one can also eliminate this region of parameter space by adding the SDSS data, which do not favor the high optical depth values (Fig. 10), and we give an example of this in Table II.

In this paper we are more interested in how running changes if we use the exact likelihood routine as opposed to the approximate one. The resulting values of the running for various cases are given in Tables I and II. They are significantly affected by the exact likelihood calculations. This is expected from the analysis presented in the previous section, where we showed that the exact likelihood analysis with foreground marginalization leads to an enhancement of low ℓ multipoles and broadens the shape of the likelihood distribution for quadrupoles to allow a higher likelihood for models with less negative running. Figure 9 shows the MCMC generated probability distributions for running α_s using WMAPext+SDSS in eight-parameter models. Note that there is a strong correlation between running and tensors in such a way that for no tensors there is less evidence for running [25]. So some of the evidence for running in the eight-parameter analysis (and in [33]) is driven simply by the large parameter space of $r>0$ models and should not be taken as evidence of running on its own. Even so we find that the evidence for running, marginally suggested by the old analysis, largely goes away in the new analysis and the value of running changes from -0.060 to -0.015 (V KP2, full marginalization) or -0.032 (W KP2, dust marginalization only), with an error of 0.035. This confirms that the sug-

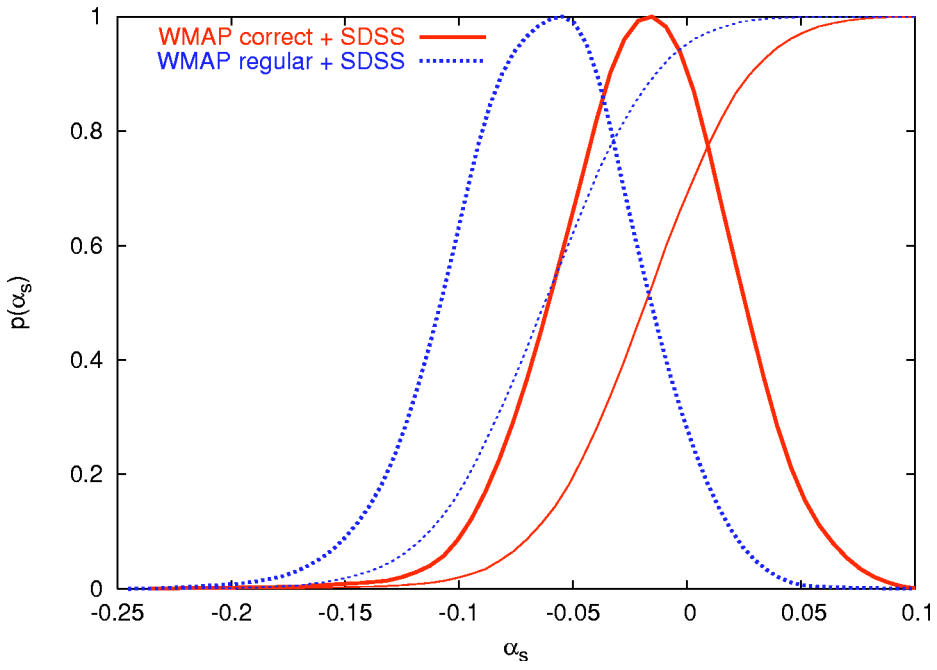

FIG. 10. Two-dimensional contours of 68% and 95% probability in (α_s,τ) and $(\alpha_s,z_{\rm ri})$ planes from WMAP+VSA and WMAP+VSA+SDSS data.

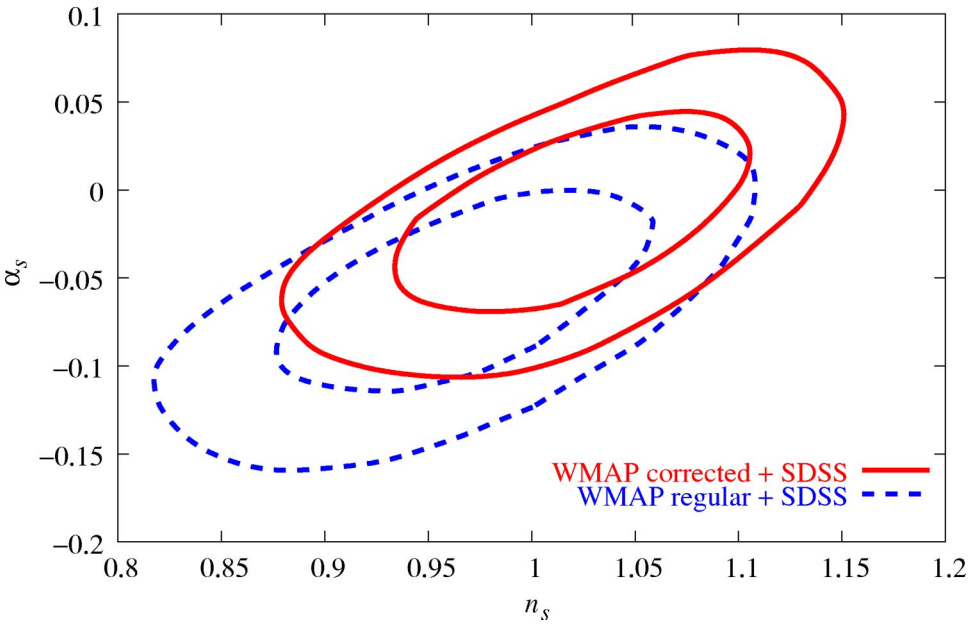

FIG. 11. Two-dimensional contours of 68% and 95% probability in (α_s, n_s) plane for old and new MCMCs using WMAPext+SDSS data. We use V frequency map and KP2 mask in the full likelihood analysis.

gested evidence for running relies crucially on a low quadrupole and octupole [34], for which the statistical analysis and foreground removal are least reliable.

This point was also noted in the recent analysis of WMAP+VSA data [32], where the WMAP likelihood code was used and evidence in excess of 2σ for running was found, while removing $\ell<10$ information reduced this evidence to less than 1σ. While one should not simply remove the entire $\ell<10$ information one should use the exact calculations instead of approximate ones if the answer depends on it. Our results for a WMAP+SDSS+VSA analysis for seven-parameter models without tensors given in Table II show that running is strongly suppressed with the new analysis, $\alpha_s=-0.022^{+0.034}_{-0.032}$, even without adopting any prior on the optical depth.

As shown in Table I the best fitted value of the primordial slope n_s increases appreciably as well, although this is mostly a consequence of the change in running. This is clarified in Fig. 11, which shows old and new contours in the (n_s, α_s) plane. There is some degeneracy between the two parameters, so that models with low values of running also require low slope. Since low values of running are excluded by the new analysis, this implies that low values of the primordial slope are also excluded, pushing the average slope up.

V. CONCLUSIONS

In this paper we have developed routines to calculate the exact likelihood of the low resolution WMAP data. We have projected out unwanted foreground components by adding the foreground templates to our covariance matrix with large variance. Neither of these methods has been applied to WMAP data before and should improve upon the existing analyses. We have tested the robustness of our results by applying the method to many different combinations of observing frequency, mask, smoothing, and templates and found consistent results among these various cases. In particular, we find consistent results if we marginalize only over dust in the W channel as opposed to all three foreground templates, if we use templates external to WMAP instead of the WMAP MEM templates, if we use the KP0 instead of the KP2 mask, if we use ILC maps instead of individual V or W frequencies, or if we use HEALPIX windows instead of Gaussian smoothing. The two most important features of our procedure are thus marginalization over dust and exact likelihood analysis.

Important differences exist between our results and previous work. We find higher values of the lowest multipoles, which is partly a consequence of the template subtraction method used in the WMAP analysis. This procedure would certainly remove some of the real power, although it is difficult to estimate how much, and the differences could also be just a statistical fluctuation. For the maximum likelihood value of the quadrupole we find values between the original WMAP analysis and subsequent reanalysis by [12]. The differences are within the estimated error of the foreground contamination, and we argue that the actual value is not very reliable given how broad the likelihood is at the peak. More important is the shape of the likelihood function, which we find to be broader than in the likelihood evaluation, provided by the WMAP team which underestimates the errors compared to our analysis. This lowers the statistical significance of the departure of the data from the concordant model. Within a Bayesian context and assuming a flat prior on the distribution of quadrupoles, we find the probability that a model exceeds the concordance model predicted quadrupole to be 10%. We also do not find anything particularly unusual in the correlation function and in the joint quadrupole-octopole analysis.

We combine the full likelihood calculation with foreground marginalization at low ℓ with the original WMAP PCL analysis at high ℓ to generate Monte Carlo Markov chains, whose distribution converges to the probability distribution of theoretical models given the data and assumed

priors. The main effect of the new analysis is on the running of the spectral index, for which the marginal 2σ evidence for $\alpha_s<0$ present in the original analysis and in the recent analysis of WMAP+VSA [32] (see also [31]) is reduced to below 1σ. Using the exact WMAP likelihood analysis will be essential for attempts to determine the running of the spectral index by combining WMAP with either the small scale CMB data or the upcoming Ly-α forest analysis from SDSS. In all of these cases the exact method increases the value of the running by pushing up the CMB spectrum at large scales. Another parameter that is significantly affected is the matter density Ω_m or, equivalently, the dark energy density Ω_Λ. We find Ω_m to be reduced by the new analysis because of the added power at low multipoles, which is most easily accounted for by an increase in the ISW contribution.

We have shown that the effects of the improved likelihood analysis presented here can be significant for the determination of cosmological parameters. We expect the methods applied here will be equally important for the analysis of polarization data in WMAP, where the foregrounds play a much more important role and where a full likelihood analysis of joint temperature and polarization data is necessary to extract the maximum amount of information. The current analysis of temperature-polarization data is rather unsatisfactory, since it is based on the cross-spectrum information alone. Without having access to the full polarization maps we cannot improve upon it here. Thus the results shown in Tables I and II should still be viewed as preliminary regarding the optical depth, which is essentially determined by the polarization data. The upcoming WMAP two-year analysis and release of polarization data should elucidate the current situation. The code developed here will be made available to the community at cosmas.org.

ACKNOWLEDGMENTS

We thank WMAP for the wonderful data they produced and made available through the LAMBDA web site. Our MCMC simulations were run on a Beowulf cluster at Princeton University, supported in part by NSF Grant No. AST-0216105. U.S. thanks O. Dore, C. Hirata, P. McDonald, and D. Spergel for useful discussions. U.S. is supported by the Packard Foundation, Sloan Foundation, NASA Grant No. NAG5-1993, and NSF Grant No. CAREER-0132953.

[1] C.L. Bennett *et al.*, Astrophys. J., Suppl. Ser. **148**, 1 (2003).
[2] E. Hivon, K.M. Górski, C.B. Netterfield, B.P. Crill, S. Prunet, and F. Hansen, Astrophys. J. **567**, 2 (2002).
[3] M. Tegmark, Phys. Rev. D **55**, 5895 (1997).
[4] J.R. Bond, A.H. Jaffe, and L. Knox, Astrophys. J. **533**, 19 (2000).
[5] L. Verde *et al.*, Astrophys. J., Suppl. Ser. **148**, 195 (2003).
[6] G. Efstathiou, Mon. Not. R. Astron. Soc. **349**, 603 (2004).
[7] D.N. Spergel *et al.*, Astrophys. J., Suppl. Ser. **148**, 175 (2003).
[8] G. Efstathiou, Mon. Not. R. Astron. Soc. **346**, L26 (2003).
[9] C.R. Contaldi, M. Peloso, L. Kofman, and A. Linde, J. Cosmol. Astropart. Phys. **7**, 2 (2003).
[10] J.M. Cline, P. Crotty, and J. Lesgourgues, J. Cosmol. Astropart. Phys. **9**, 10 (2003).
[11] B. Feng and X. Zhang, Phys. Lett. B **570**, 145 (2003).
[12] G. Efstathiou, Mon. Not. R. Astron. Soc. **348**, 885 (2004).
[13] C.L. Bennett *et al.*, Astrophys. J., Suppl. Ser. **148**, 97 (2003).
[14] C.G.T. Haslam, H. Stoffel, C.J. Salter, and W.E. Wilson, Astron. Astrophys., Suppl. Ser. **47**, 1 (1982).
[15] D.P. Finkbeiner, Astrophys. J., Suppl. Ser. **146**, 407 (2003).
[16] D.J. Schlegel, D.P. Finkbeiner, and M. Davis, Astrophys. J. **500**, 525 (1998).
[17] M. Tegmark, A. de Oliveira-Costa, and A.J. Hamilton, Phys. Rev. D **68**, 123523 (2003).
[18] H.K. Eriksen, A.J. Banday, K.M. Gorski, and P.B. Lilje, astro-ph/0403098.
[19] J.R. Bond, A.H. Jaffe, and L. Knox, Phys. Rev. D **57**, 2117 (1998).
[20] G.B. Rybicki and W.H. Press, Astrophys. J. **398**, 169 (1992).
[21] K. M. Górski, A. J. Banday, E. Hivon, and B. D. Wandelt, in *Astronomical Data Analysis Software and Systems XI*, ASP Conference Series Vol. 281 (2002), p. 107.
[22] G. Hinshaw *et al.*, Astrophys. J., Suppl. Ser. **148**, 135 (2003).
[23] U. Seljak and M. Zaldarriaga, Astrophys. J. **469**, 437 (1996).
[24] A. Gelman and D. Rubin (unpublished).
[25] U. Seljak, P. McDonald, and A. Makarov, Mon. Not. R. Astron. Soc. **342**, L79 (2003).
[26] B.S. Mason *et al.*, Astrophys. J. **591**, 540 (2003).
[27] C.L. Kuo *et al.*, Astrophys. J. **600**, 32 (2004).
[28] M. Tegmark *et al.*, astro-ph/0310725.
[29] C. Dickinson *et al.*, astro-ph/0402498.
[30] W.L. Freedman *et al.*, Astrophys. J. **553**, 47 (2001).
[31] A.C.S. Readhead *et al.*, astro-ph/0402359.
[32] R. Rebolo *et al.*, astro-ph/0402466.
[33] H.V. Peiris *et al.*, Astrophys. J., Suppl. Ser. **148**, 213 (2003).
[34] S.L. Bridle, A.M. Lewis, J. Weller, and G. Efstathiou, Mon. Not. R. Astron. Soc. **342**, L72 (2003).